Bull. Mater. Sci., Vol. 35, No. 3, June 2012, pp. 369–376. © Indian Academy of Sciences.

Controlled synthesis and electrochemical properties of vanadium oxides with different nanostructures

YIFU ZHANG, MEIJUAN FAN†, MIN ZHOU, CHI HUANG, CHONGXUE CHEN, YULIANG CAO, GUANGYONG XIE‡,*, HOUBIN LI† and XINGHAI LIU†

College of Chemistry and Molecular Sciences, Wuhan University, Wuhan 430072, P.R. China

†School of Printing and Packaging, Wuhan University, Wuhan 430079, P.R. China

‡Key Laboratory of Catalysis and Materials Science of the State Ethnic Affairs Commission & Ministry of Education, College of Chemistry and Materials Science, South-Central University for Nationalities, Wuhan 430074, P.R. China

MS received 15 July 2011; revised 13 August 2011

Abstract. **Vanadium oxides ($V_3O_7{\cdot}H_2O$ and VO_2) with different morphologies have been selectively synthesized by a facile hydrothermal approach using glucose as the reducing and structure-directing reagent. The as-obtained $V_3O_7{\cdot}H_2O$ nanobelts have a length up to several tens of micrometers, width of about 60–150 nm and thickness of about 5–10 nm, while the as-prepared VO_2(B) nanobelts have a length of about 1·0–2·7 μm, width, 80–140 nm and thickness, 2–8 nm. It was found that the quantity of glucose, the reaction temperature and the reaction time had significant influence on the compositions and morphologies of final products. Vanadium oxides with different morphologies were easily synthesized by controlling the concentration of glucose. The formation mechanism was also briefly discussed, indicating that glucose played different roles in synthesizing various vanadium oxides. The phase transition from VO_2(B) to VO_2(M) were investigated and the phase transition temperature of the VO_2(M) appeared at around 68 °C. Furthermore, the electrochemical properties of $V_3O_7{\cdot}H_2O$ nanobelts, VO_2(B) nanobelts and VO_2(B) nanosheets were investigated and they exhibited a high initial discharge capacity of 296, 247 and 227 mAh/g, respectively.**

Keywords. **Vanadium oxides; nanostructured materials; chemical synthesis; electrochemical property; VO_2(M).**

1. Introduction

In the past decade, much attention has been paid on low dimensional nanomaterials with novel morphologies including nanobelts, nanotubes, nanowires, nanosheets, etc. They exhibit specific physical and chemical properties and wide potentials in nanodevices, which are different from their bulk materials (Fasol 1998; Zhong *et al* 2003; Wu *et al* 2004; Hu *et al* 2007; Wang *et al* 2007). It was reported that the electrochemical properties of the batteries depend not only on the structure, but also on the morphology of the electrode components (Huynh *et al* 2002). It was shown that 1D nanostructures are more prone to charge transport than the bulk crystalline structures. Therefore, to synthesize materials with nanostructures is very meaningful and a challenge for materials scientists.

Of the family of metal oxides, vanadium oxides and their derived compounds as functional materials have received extensive attention because of their structures, novel electronic and optical properties, which make them have a wide range of practical applications, such as catalyst, gas sensor, cathode materials for reversible lithium batteries, electrochemical and optical devices, intelligent thermochromic windows, and so on (Chatterjee *et al* 2001; Parkin and Manning 2006; Rao *et al* 2006; Gao *et al* 2009; Strelcov *et al* 2009; Ye *et al* 2010). Vanadium usually forms a variety of binary oxides with the general formula, VO_{2+x} ($-0{\cdot}5 \leq x \leq 0{\cdot}5$), such as V_2O_3, VO_2, V_2O_5, V_3O_7, V_4O_9, V_6O_{13}. Recently, vanadium oxide hydrate, $V_3O_7{\cdot}H_2O$ and vanadium oxide, VO_2(B), have attracted more and more attention due to their specific magnetism, catalyst and electrochemistry (Hironori *et al* 1979; Liu *et al* 2004; Feyel *et al* 2006; Dong *et al* 2008). Therefore, several methods such as thermal decomposition (Michel *et al* 1973; Odani *et al* 2006), chemical vapour deposition (Su *et al* 2009), surfactant assisted approach (Shi *et al* 2007; Zhou *et al* 2007), templates methods (Yu and Zhang 2004; Sediri and Gharbi 2009), hydrothermal/solvothermal routes (Liu *et al* 2004; Liu X *et al* 2007; Liu X H *et al* 2007), etc, have been developed to synthesize VO_2(B) or $V_3O_7{\cdot}H_2O$ with nanostructures. Among above methods, the hydrothermal method has been receiving increasing attention because of its uncomplicated route. However, as far as we know, few reports focused on the synthesis of different vanadium oxides with different morphologies in a single system by the hydrothermal method. Therefore, it is significant to prepare different vanadium oxides with novel structures using V_2O_5 as starting material because it is the cheapest commercial

*Author for correspondence (xxgyy@hotmail.com)

vanadium compound. Although glucose and V_2O_5 (molar ratio = 1:1) as the starting regents were reported to synthesize VO_2(B) nanobelts at 180 °C for 24 h (Li *et al* 2010), the synthesis of $V_3O_7{\cdot}H_2O$ nanobelts and VO_2(B) nanosheets were not studied. Besides, thickness of the as-synthesized nanobelts in our results was much thinner than the results reported by Li *et al* (2010). To the best of our knowledge, it is the first time a systematic study of the synthesis of vanadium oxides with different morphologies using V_2O_5 and glucose by the hydrothermal method is reported. The quantity of glucose has great influence on the synthesis of these vanadium oxides, which is discussed in detail in this paper.

2. Experimental

2.1 *Synthesis of different vanadium oxides with different morphologies*

All the chemicals used in this work were of analytical grade. In a typical synthesis, a range of 0∼2·20 g of D–(+)–Glucose and 0·91 g of V_2O_5 powder were dispersed into 30 mL of deionized water with magnetic stirring for 5 min. And then, the mixture was transferred into a 40 mL stainless steel autoclave. The autoclave was sealed and maintained at 60–250 °C for 1–48 h and then cooled to room temperature naturally. The resulting products were filtered off, washed with distilled water and absolute ethanol several times to remove any possible residues, and dried in vacuum at 75 °C for future characterization.

2.2 *Characterization*

The purity and crystalline structure of the resulting products were investigated by X-ray powder diffraction (XRD, D8 X-ray diffractometer equipment with Cu Kα radiation, λ = 1·54060 Å). X-ray photoelectron spectroscopy (XPS, VGESCALAB MK II with Mg Kα, 1253·6 eV) was used to confirm the oxidation state of vanadium. Fourier transform infrared spectroscopy (FT–IR) pattern was recorded on a Nicolet 60–SXB spectrometer from 4000–400 cm^{-1} with a resolution of 4 cm^{-1}. Thermogravimetric analysis (TGA) was performed on SETSYS–1750 (AETARAM Instruments). About 10 mg of the as-obtained samples were heated in an Al_2O_3 crucible in nitrogen atmosphere from ambient temperature to 600 °C at a constant rate of temperature (10 °C/min). The morphology and dimension of the products were observed by scanning electron microscopy (SEM, Quanta 200), transmission electron microscopy (TEM, JEM–100CXII), and selected area electron diffraction (SAED, JEOL 2010). The samples used for characterization were dispersed in absolute ethanol and were ultrasonicated before TEM and SAED.

2.3 *Electrochemical measurements*

The electrochemical properties of samples were tested in assembling experiment cells with metallic lithium as the negative electrode. The working electrode was made by dispersing with 85 wt % active materials (the as-obtained vanadium oxides), 10 wt % acetylene back carbon powder, and 5 wt % polyvinylidene fluoride (PVDF) binder in *N*-methyl-2-pyrrolidone (NMP) solvent to form a homogeneous slurry. The slurry was then spread and pressed on Al foil. The coated electrodes were dried in vacuum at 125 °C for 18 h. The electrolyte was 1 $mol{\cdot}L^{-1}$ $LiPF_6$ in a mixture of ethylene carbonate (EC) and diethyl carbonate (DEC) (EC/DEC = 1/1, v/v). The cells were assembled in a glove box under an argon atmosphere. Charge–discharge tests were carried out in a voltage range of 4·0–1·5 V and current density of 0·2 mA/cm^2.

3. Results and discussion

The synthetic conditions, the crystalline phases, and the morphologies of shape-controlled orthorhombic $V_3O_7{\cdot}H_2O$ and monoclinic VO_2(B) materials are mainly summarized in table 1. In this paper, $V_3O_7{\cdot}H_2O$ and VO_2(B) materials are synthesized using V_2O_5 as the starting vanadium source and glucose (0–3·20 g) as the reducing and structure-directing reagent by a facile hydrothermal approach at 60–250 °C for 1–48 h. In our synthetic routes, neither surfactant nor other reagent is used. It is well known that the hydroxyl group has certain reducibility at the hydrothermal conditions (Liu X H *et al* 2007; Zhang *et al* 2010) and the number of hydroxyl groups (–OH) is 5 in glucose. Therefore, V_2O_5 can be reduced by glucose and the phases and morphologies of

Table 1. Synthesis conditions, crystal phases and morphologies of the as-synthesized vanadium oxides[a].

Sample	Glucose (g)	Temperature (°C)	Time	Product	Morphology
1.	0·067	150–180	12–48	$V_3O_7{\cdot}H_2O$	Regular nanobelts
2.	0·198	180	12	$V_3O_7{\cdot}H_2O$ and VO_2(B)	Long and short nanobelts
3.	0·267	150	12	VO_2(B)	Short and irregular nanobelts
4.	0·267	180	12	VO_2(B)	Nanobelts
5.	0·267	180	48	VO_2(B) and VO_2(B)@C	Nanobelts, core-shell structure
6.	1·60	180	12	VO_2(B) and carbon	Nanosheets and carbon sphere
7.	2·20	150	12	VO_2(B) and carbon	Nanosheets, nanofibres and carbon sphere

[a]All samples were synthesized by hydrothermal process with 0·91 g of V_2O_5 and 30 mL of water.

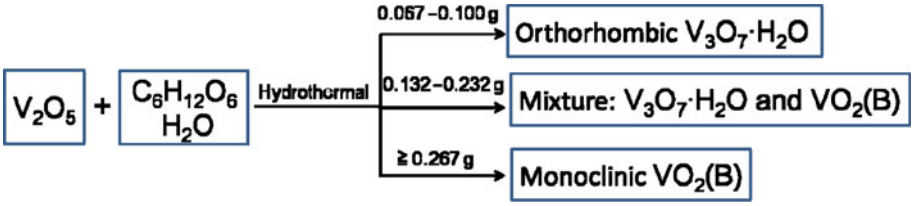

Scheme 1. General synthetic procedure for controlled synthesis of different vanadium oxides.

the final products can be controlled by the quantity of glucose in our synthetic routes.

The procedure for the synthesis of these materials at 150–180 °C for 12 h is illustrated in scheme 1. $V_3O_7{\cdot}H_2O$ nanobelts were synthesized at a relatively low quantity of glucose (0·067–0·100 g). With the amount of glucose increased, much vanadium in the +5 valence state was reduced to +4 valence state. Finally, VO_2(B) nanobelts were obtained with a relatively high quantity of glucose ($\geqq$ 0·267 g). These results (discussed in the following section) indicate that phases and morphologies of vanadium oxides can be easily controlled by only changing the quantity of glucose. A series of glucose-dependent experiments were performed to understand the formation of vanadium oxides nanostructures. The synthetic reactions were carried out with different quantities of glucose (0, 0·033, 0·067, 0·100, 0·132, 0·165, 0·198, 0·232, 0·267, 0·334, 0·395, 0·790, 1·60 and 3·20) for 12 h and each experiment used the same starting chemical composition mixture (i.e. 0·91 g of V_2O_5 and 30 mL of H_2O). The suitable conditions to synthesize $V_3O_7{\cdot}H_2O$ nanobelts are as follows: 0·067–0·100 g of glucose, at 150–180 °C for 12 h, while favourable conditions for VO_2(B) are 0·267 g of glucose, at 180 °C for 12 h.

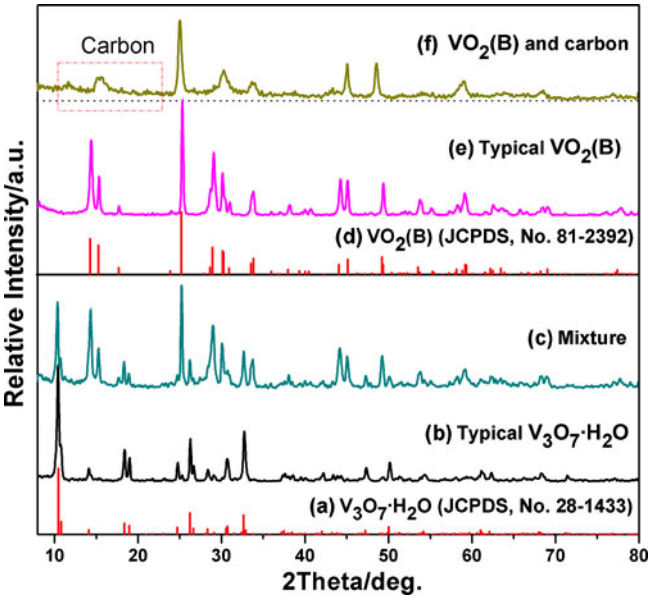

Figure 1. XRD patterns of typical orthorhombic $V_3O_7{\cdot}H_2O$ and monoclinic VO_2(B) nanobelts synthesized using different quantities of glucose: (**b**) 0·067 g; (**c**) 0·232 g; (**e**) 0·267 g; (**f**) 1·60 g. (Reaction conditions: 0·91 g of V_2O_5, 30 mL of H_2O and at 180 °C for 12 h).

3.1 *Characterization of typical orthorhombic $V_3O_7{\cdot}H_2O$ nanobelts and monoclinic VO_2(B) nanobelts*

The typical orthorhombic $V_3O_7{\cdot}H_2O$ and monoclinic VO_2(B) nanobelts were characterized by XRD, SEM, TEM, SAED, XPS, FT–IR and TGA measurements. Figure 1b represents typical XRD pattern of $V_3O_7{\cdot}H_2O$ nanobelts obtained with 0·067 g of glucose used in the experiment. All the diffraction peaks from figure 1b can be readily indexed as orthorhombic crystalline phase of $V_3O_7{\cdot}H_2O$ with the calculated lattice constant $a = 9{\cdot}381$, $b = 16{\cdot}881$, $c = 3{\cdot}635$ Å, which corresponds to the $V_3O_7{\cdot}H_2O$ (JCPDS No. 28–1433) already described in the literature (Theobald and Cabala 1970). No peaks of any other phases are detected from the XRD pattern, indicating as-prepared $V_3O_7{\cdot}H_2O$ nanobelts with high purity. However, a mixture of $V_3O_7{\cdot}H_2O$ and VO_2(B) is obtained when the amount of glucose increased to 0·232 g, as shown in figure 1c. Figure 1e depicts typical XRD pattern of VO_2(B) nanobelts synthesized with 0·267 g of glucose. In a similar method, all the diffraction peaks from the XRD pattern can be readily indexed as the monoclinic crystalline phase (space group $C2/m$) of VO_2(B) with calculated lattice constant $a = 12{\cdot}067$, $b = 3{\cdot}694$, $c = 6{\cdot}431$ Å, $\beta = 106{\cdot}84$, which corresponds to VO_2(B) (JCPDS, No. 81–2392) already described in the literature (Oka *et al* 1993). The as-prepared VO_2(B) nanobelts are of high purity because no peaks of any other phases are detected from the XRD pattern. With the amount of glucose increased to 1·60 g, the main phase of the sample is VO_2(B), as shown in figure 1f. But some peaks do not appear and the background ranging from 10° to 20° is slightly bulged, indicating that a new phase might exist (organic carbon) (Sun *et al* 2006; Xuan *et al* 2007), which is verified by TEM and FT–IR discussed in the following section.

Furthermore, composition and vanadium valence state of the surface of the typical $V_3O_7{\cdot}H_2O$ and VO_2(B) nanobelts were investigated by XPS test, as shown in figure S1 (supplementary data). The survey spectrums (figures S1a and S1c) reveal both $V_3O_7{\cdot}H_2O$ and VO_2(B) only consist of vanadium and oxygen. The high resolution XPS region spectrum confirms that $V_3O_7{\cdot}H_2O$ consist of V(V) and V(IV), while VO_2(B) contains V(IV). To get more information about the structure of $V_3O_7{\cdot}H_2O$ nanobelts, the corresponding FT–IR and TG measurements were carried out. The results are shown in figure S2 (supplementary data).

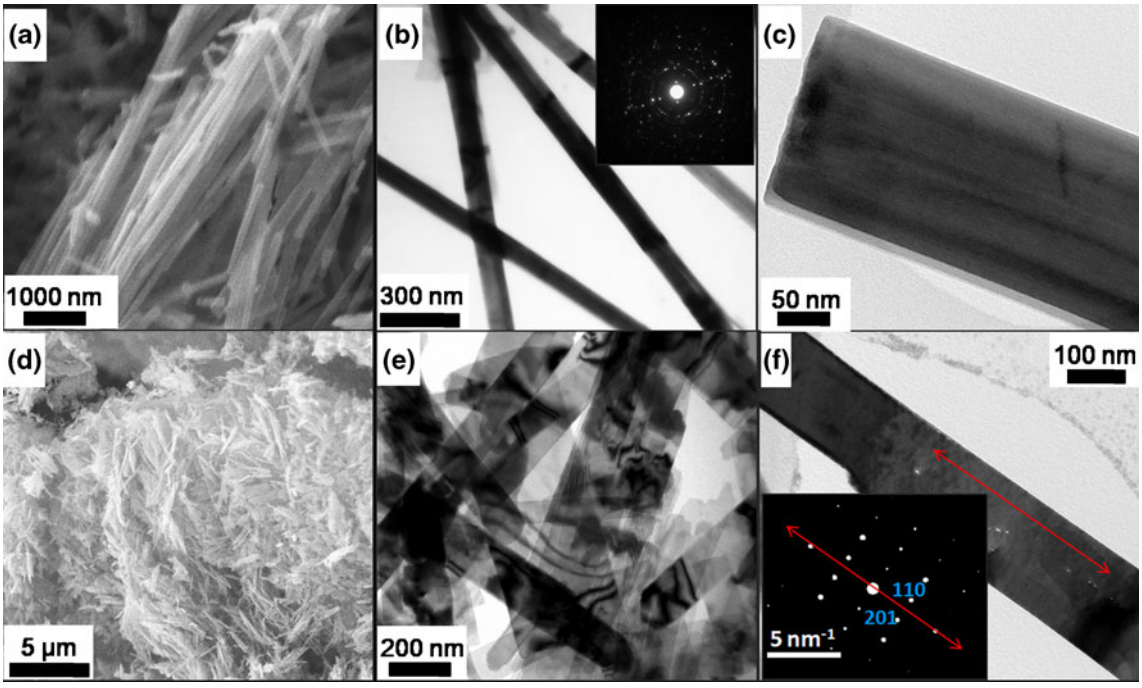

Figure 2. TEM images of typical products: (**a–c**) orthorhombic $V_3O_7{\cdot}H_2O$ nanobelts (0·067 g of glucose, 150 °C); (**d–f**) monoclinic (0·267 g of glucose, 180 °C).

The morphologies and structures of the typical $V_3O_7{\cdot}H_2O$ and VO_2(B) nanobelts were investigated by SEM and TEM measurements, as shown in figure 2. Figures 2a–c reveal that it consists of a large quantity of $V_3O_7{\cdot}H_2O$ nanobelts with length up to several tens of micrometers, width of about 60–150 nm and thickness of about 5–10 nm (clearly seen from figure 2c). From figures 2b–c, we can infer that the products are independent nanobelts with smooth surface and polycrystalline electron diffraction pattern (inset of figure 2b) reveals the resulting nanobelts to be well crystallized. Figures 2d–f represent SEM and TEM photographs of VO_2(B), which describe the as-obtained VO_2(B) with length of about 1·0–2·7 μm, width, 80–140 nm and thickness, 2–8 nm, which is much thinner than the previous report (Li *et al* 2010). From figure 2d, we can see that the as-synthesized VO_2(B) are flexible. The SAED pattern (inset of figure 2f) from an individual nanobelt reveals that it is well crystallized and the growth direction of nanobelts is along [010].

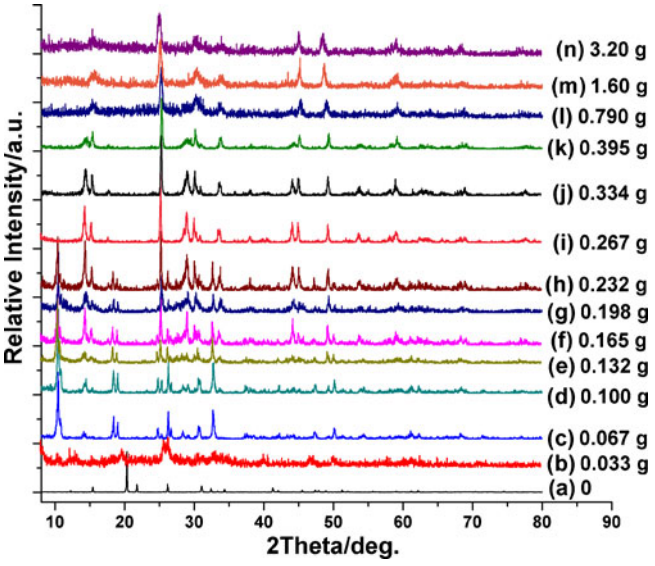

Figure 3. XRD patterns of vanadium oxides nanostructures synthesized with different quantities of glucose. (Reaction conditions: 0·91 g of V_2O_5, 30 mL of H_2O and at 180 °C for 12 h).

3.2 *Some parameters controlling phase and morphology of resulting products*

The reaction temperature and reaction time are significant factors for preparing the vanadium oxides with different morphologies. The results indicate that the temperature at 150–180 °C for 12 h is favourable for the fabrication of orthorhombic $V_3O_7{\cdot}H_2O$ nanobelts, while the favourable temperature is 180 °C for 12 h for preparing regular VO_2(B) nanobelts. The detailed discussion is represented in figures S3–S12.

The phase and morphology of vanadium oxides can be easily controlled by only changing the quantity of glucose. A series of glucose-dependent experiments were conducted to understand the formation of vanadium oxides micro/nanostructures. The synthesis reactions were carried out with different quantities of glucose (0, 0·033, 0·067, 0·100, 0·132, 0·165, 0·198, 0·232, 0·267, 0·334, 0·395, 0·790, 1·60 and 3·20) at 180 °C for 12 h and each

experiment used the same starting chemical composition mixture (i.e. 0·91 g of V_2O_5 and 30 mL of H_2O). The XRD patterns and TEM images of the vanadium oxides were obtained with different quantities of glucose at 180 °C for 12 h, while keeping other synthetic conditions unchanged and are shown in figures 3 and 4. For the sample prepared without glucose, only V_2O_5 was obtained (figure 3a), which means glucose should play the role of reducer in our system. When 0·033 g of glucose was added to the system, the resulting products of the mixture (figure 3b) and many sheets were also seen in figure 4a. Simultaneously, some very short belt-like structures which might be the precursor of the $V_3O_7{\cdot}H_2O$ nanobelts appeared. The reason given was that they were restrained in growing into high-aspect-ratio nanobelts due to the lack of vanadium in +4 oxidation state in the system. Low-valence vanadium oxides were synthesized using glucose as the reducing reagent. With the quantity of glucose increased, the final products were from $V_3O_7{\cdot}H_2O$ to VO_2(B). However, V_2O_3 could not be obtained even with excess glucose (such as 3·20 g) used, which should be due to the reducibility of glucose. When 0·067 and 0·100 g of glucose were used, $V_3O_7{\cdot}H_2O$ nanobelts were synthesized (figures 3c–d and 4b–c). A lot of vanadium in the +5 oxidation state was reduced to that of +4 oxidation state with 0·165–0·232 g of glucose used, so the mixture of $V_3O_7{\cdot}H_2O$ and VO_2(B) was synthesized, as shown in figures 3e–h. Figure 1c represented a typical mixture ($V_3O_7{\cdot}H_2O$ and VO_2) obtained with 0·232 g of glucose. The morphologies of the mixture were irregular as depicted in figure 4d. Regular VO_2(B) nanobelts were synthesized with 0·267 g of glucose, which had been discussed in the above section (figures 2d–f). With the increase of glucose to 0·334 g or more, only VO_2(B) was obtained, and V_2O_3 could not be detected by XRD tests (figures 3j–n), but the morphology was dramatically changed. When 0·395 g of glucose was used, short and broken belts were synthesized (figure 4e), while a great number of nanosheets were fabricated when the amount of glucose increased to 1·60 g (figure 4f).

Keeping other synthetic conditions unchanged and lowering the reaction temperature (150 °C), we can get similar results. Their corresponding XRD patterns and TEM images are, respectively shown in figures S13 and S14. Note that very regular $V_3O_7{\cdot}H_2O$ nanobelts are synthesized at 150 °C (figures S14b and c) with 0·067 g of glucose used. A number of nanosheets of VO_2(B) were fabricated with 2·20 g of glucose added in our experiment (figures S14g–h). What is more, some nanofibres were occasionally seen at this condition, as shown in figures S14i and j.

3.3 *Formation mechanism for synthesizing vanadium oxides*

On the basis of the above results, vanadium oxides with different phases were synthesized by the defined interval: $V_3O_7{\cdot}H_2O$ (glucose: 0·07–0·10 g) and VO_2(B) (glucose: 0·27 g or more) at 150–180 °C for 12 h. With the increase of glucose, the morphologies of the as-obtained vanadium oxides are dramatically different, which can be

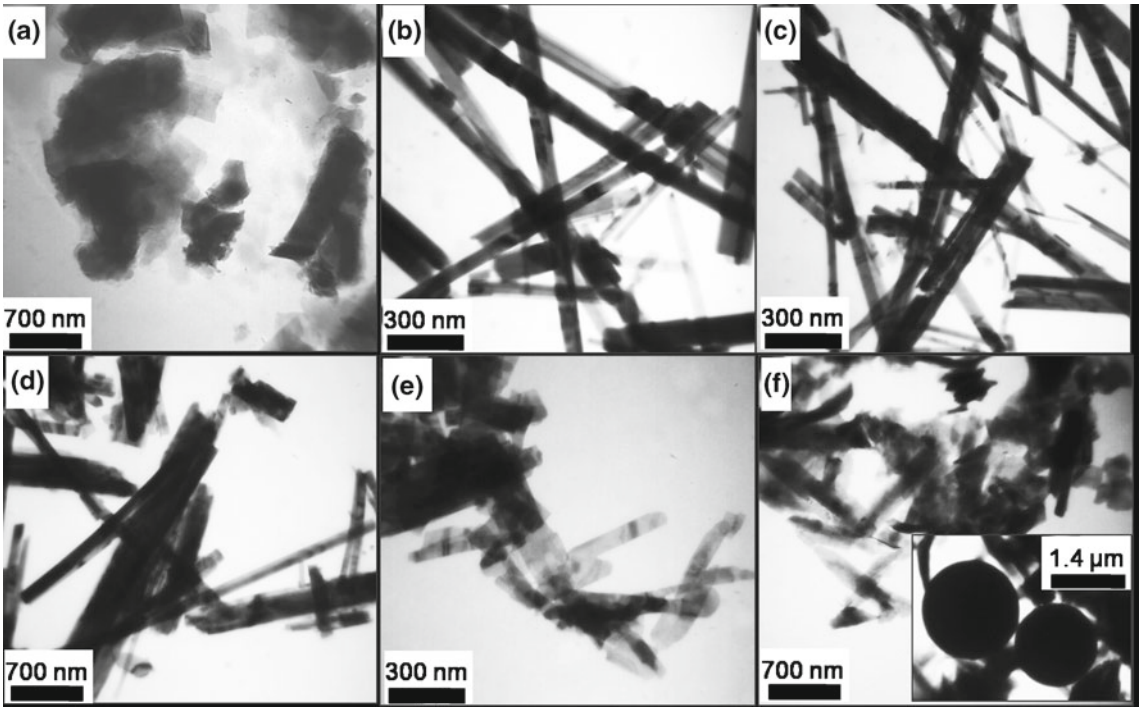

Figure 4. TEM images of vanadium oxides nanostructures synthesized with different quantities of glucose: (**a**) 0·033 g; (**b**) 0·067 g; (**c**) 0·100 g; (**d**) 0·198 g; (**e**) 0·395 g; (**f**) 1·60 g. (Reaction conditions: 0·91 g of V_2O_5, 30 mL of H_2O and at 180 °C for 12 h).

due to the effect of glucose. When a small amount of glucose was utilized (for the synthesis of $V_3O_7{\cdot}H_2O$), the main effect of glucose is as the reductant and the formation of $V_3O_7{\cdot}H_2O$ nanobelts is probably due to the intrinsic growth habit of $V_3O_7{\cdot}H_2O$, which is supported by the result that $V_3O_7{\cdot}H_2O$ nanobelts were synthesized by replacing glucose with ethanol in the experiment by our team (Zhang *et al* 2010). Therefore, the formation mechanism of synthesizing $V_3O_7{\cdot}H_2O$ nanobelts can be described as "hydrating–reducing–exfoliating–splitting" (HRES) mechanism, which has been proposed in our previous report (Zhang *et al* 2010). This mechanism mainly contains four steps as follows: (i) the raw material of V_2O_5 is hydrated to form $V_2O_5{\cdot}xH_2O$ which is more active and is easily reduced by glucose; (ii) $V_2O_5{\cdot}xH_2O$ is reduced to $V_3O_7{\cdot}H_2O$ with layered structure by glucose; (iii) the hydrated vanadium oxides ($V_3O_7{\cdot}H_2O$) with layered structure are exfoliated to nanosheets under the drives of inter tension and crystal growth anisotropy; (iv) the nanosheets are further split into nanobelts. The reducing ability in the system is strengthened with increase in quantity of glucose, resulting in the synthesis of the phase of VO_2(B). However, the morphologies of VO_2(B) are as follows: uniform nanobelts (figures 2d–f), the short and broken belts (figure 4e), and sheets (figure 4f). These results might be attributed to two reasons. First, the byproducts of glucose affected the formation of VO_2(B) nanobelts with comparatively less glucose used (such as 0·267 g), but the effect was limited because VO_2(B) nanobelts were finally formed. Second, with excess glucose added to the system, the residual glucose could be crosslinked with each other to form carbon sphere (figure 4f, inset) (Sun and Li 2004) to prevent irregular vanadium dioxides growing into regular nanobelts, resulting in obtaining VO_2(B) nanosheets. This speculation was proved by FTIR as seen in figure 5. The peaks at 1710 cm^{-1} and 1601 cm^{-1} were attributed to C=O and C=C stretches, respectively. The transmittance of C=O was comparatively weak, which might imply that the number of C=O bond was much fewer than that of C=C in the carbon sphere. The wavenumbers from 2950–2800 cm^{-1}, were the characteristic C–H stretches. The peaks at 998 cm^{-1} and 545 cm^{-1} were assigned to V^{4+}=O and V–O–V, respectively.

3.4 *Phase transition from VO_2(B) to VO_2(M)*

Since the discovery by Morin (1959), that the metal–semiconductor transition temperature of VO_2(M) is close to room temperature, many researchers have devoted their interest to synthesis and application of VO_2. Until now, VO_2 was being used in many areas (Hood and De Natale 1991; Li *et al* 1994; Sella *et al* 1998; Lopez *et al* 2001; Parkin and Manning 2006; Kim *et al* 2007), such as temperature sensing devices, optical switching devices, optical or electrical modulators, rechargeable lithium batteries, optical data storage media, intelligent thermochromic windows, uncooled infrared detectors, etc. From the literature investigated, the methods of synthesizing VO_2(M) are commonly treated by other phase of VO_2 with high temperature at inert atmosphere. Therefore, in this paper, we investigated the transition from VO_2(B) to VO_2(M) by thermal treatment and the metal–semiconductor transition of VO_2(M). The hydrothermal VO_2(B) was heated in a tube furnace with 5 °C/min heating rate under a flow of nitrogen gas at 700 °C for 2 h, and then cooled to room temperature in the nitrogen flow to prevent oxidation of vanadium dioxide. VO_2(M) solids were obtained through phase transition. Figure 6 represents XRD and DSC results of the VO_2(M). All the diffraction peaks from figure 6 can be readily indexed as monoclinic crystalline phase (space group: $P21/c$) of VO_2(M), which corresponds to the VO_2(M) (JCPDS No. 72–514, a = 5·74300, b = 4·51700, c = 5·37500 Å) already described in the literature (Andersson 1956). No peaks of any other phases are detected from the XRD pattern, indicating the as-prepared VO_2(M) with high purity. The phase transition temperature

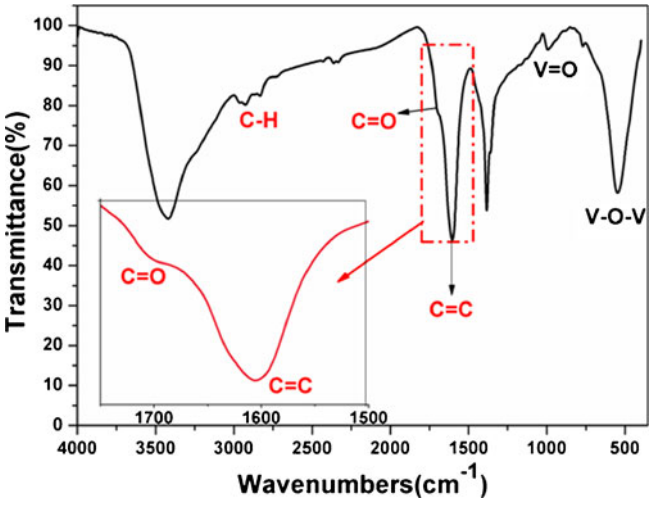

Figure 5. FT–IR spectrum of sample obtained with 1·60 g of glucose.

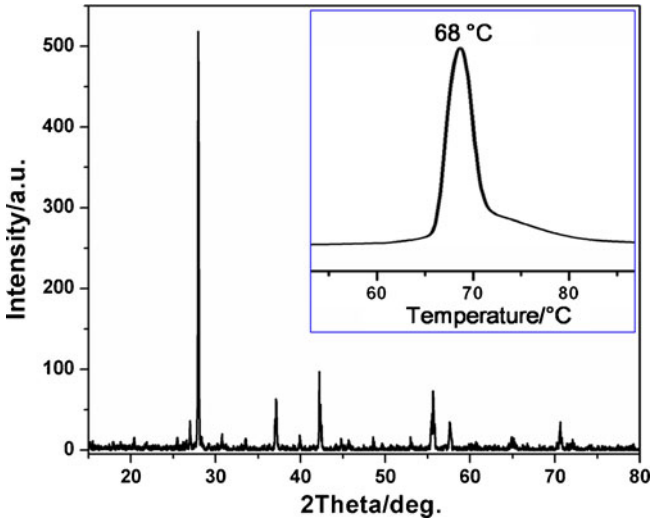

Figure 6. XRD pattern of VO_2(M) (inset: a DSC curve of VO_2(M)).

of the sample was investigated by DSC (inset of figure 6). The endothermic peak representing the phase transition temperature of the as-obtained VO_2(M) appeared at 68 °C on the curve, in accordance with the result reported by Morin (1959).

3.5 *Electrochemical properties*

In past decades, the vanadium oxides (such as VO_2, V_2O_5, V_3O_7, V_6O_{13}) with layered structure and their doped materials have attracted much attention, especially as an electrode for electrochemical applications. It was reported that the electrochemical properties of the electrode materials are influenced by many factors such as instinctive structure, morphology, preparation methods, etc. Thus, in this paper, we have investigated the charge–discharge capability of samples obtained by the hydrothermal approach. Figure 7 summarizes the relationship between the cycle performance of specific capacity and the cycle number for an electrode composed of different vanadium oxides in a voltage range of 4·0–1·5 V and under a constant current density of 0·2 mA/cm^2. The $V_3O_7{\cdot}H_2O$ nanobelts, VO_2(B) nanobelts and VO_2(B) nanosheets exhibit an initial discharge capacity of as high as 296, 247, 227 mAh/g, respectively which is much higher than the values in the references reported for 1D nanomaterials like VO_2 and V_2O_5 (Sun *et al* 2004; Li *et al* 2007). The as-synthesized vanadium oxides with an initial high discharge capacity might be attributed to the large surface area and short diffusion distance resulting from the nanostructures (Wang *et al* 2005; Ng *et al* 2007). Nevertheless, with the increase in cycling numbers, a drastic electrochemical degradation was observed. They retained about 27%, 22% and 45%, respectively of the initial discharge capacity after 10 cycles and reached a relatively stabilized capacity of about 78·6, 55·6 and 102·8 mAh/g, which might be due to the

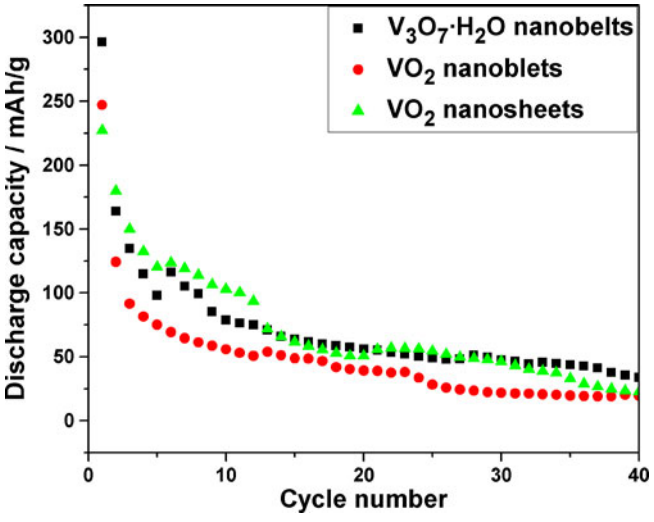

Figure 7. Cycle performance of capacitances of as-obtained vanadium oxides with different morphologies.

binder water in $V_3O_7{\cdot}H_2O$ nanobelts. The decrease of discharge capacity of the samples is probably due to partial fracture of its shape and structural degradation after redox cycle, which has been studied during the charge–discharge process of other vanadium nanostructures (Patzke *et al* 2002). All the results discussed above from the electrochemical investigation reveal that the electrochemical properties relate to the crystal structure and morphology of the electrode material, in agreement with the previous reports (Patzke *et al* 2002; Shi *et al* 2007).

4. Conclusions

In summary, we have demonstrated a facile route to synthesize large-scale vanadium oxides ($V_3O_7{\cdot}H_2O$ and VO_2) with different morphologies using commercial V_2O_5 powder as a precursor and glucose as the reducing and structure-directing reagent. The as-obtained $V_3O_7{\cdot}H_2O$ nanobelts have a length up to several tens of micrometers, width of about 60–150 nm and thickness of about 5–10 nm, while the resulting VO_2(B) nanobelts with a length of about 1·0–2·7 μm, width, 80–140 nm and thickness, 2–8 nm. Some parameters, such as the quantity of glucose, the reaction temperature and the reaction time had significant effects on the compositions and morphologies of final products. Vanadium oxides with different morphologies were obtained by controlling the concentration of glucose, and the formation process was also briefly discussed, indicating that glucose played different roles in synthesizing various vanadium oxides with different morphologies. VO_2(B) can be converted into VO_2(M) by heating up to 700 °C, whose metal semiconductor transition temperature is around 68 °C. Finally, the as-obtained $V_3O_7{\cdot}H_2O$ nanobelts, VO_2(B) nanobelts and VO_2(B) nanosheets which exhibit high initial discharge capacity of 296, 247, 227 mAh/g, respectively are promising cathode materials in lithium–ion batteries tested by the electrochemical measurements, indicating that these materials may have potential application in the future.

Electronic supplementary material

Supplementary material pertaining to this article is available on the Bulletin of Materials Science Website: www.ias.ac.in/matersci

Acknowledgements

This work was partially supported by the Fundamental Research Funds for the Central Universities, the Fourth Installment of Science and Technology Development 2010 Program of Suzhou (SYG201005), Independent Research Projects of Wuhan University (217274721) and Luojia Young Scholars Program (217273483). We thank Mr Shaobo Mo, Mr Weibing Wu, and Mrs Ling Hu for help in TEM, FT–IR, TG, XRD and SAED measurements.

References

Andersson G 1956 *Acta Chem. Scand.* **10** 623

Chatterjee P, Sen Gupta S P and Sen S 2001 *Bull. Mater. Sci.* **24** 173

Dong F, Heinbuch S, Xie Y, Rocca J J, Bernstein E R, Wang Z -C, Deng K and He S -G 2008 *J. Am. Chem. Soc.* **130** 1932

Fasol G 1998 *Science* **280** 545

Feyel S, Schroder D, Rozansk X, Sauer J and Schwarz H 2006 *Angew. Chem. Int. Ed.* **45** 4677

Gao S, Chen Z, Wei M, Wei K and Zhou H 2009 *Electrochim. Acta* **54** 1115

Hironori N, Yutaka U, Koji K, Hiroshi Y and Sukeji K 1979 *J. Phys. Soc. Jpn* **47** 790

Hood P J and DeNatale J F 1991 *J. Appl. Phys.* **70** 376

Hu C, Liu H, Dong W, Zhang Y, Bao G, Lao C and Wang Z L 2007 *Adv. Mater.* **19** 470

Huynh W U, Dittmer J J and Alivisatos A P 2002 *Science* **295** 2425

Kim B J, Lee Y W, Chae B G, Yun S J, Oh S Y, Kim H T and Lim Y S 2007 *Appl. Phys. Lett.* **90** 023515

Li J, Su Z, Yang B, Cai S, Dong Z, Man J and Li R 2010 *J. Phys. Chem. Solids* **71** 407

Li W, Dahn J R and Wainwright D S 1994 *Science* **264** 1115

Li X, Li W, Ma H and Chen J 2007 *J. Electrochem. Soc.* **154** A39

Liu J F, Li Q H, Wang T H, Yu D P and Li Y D 2004 *Angew. Chem. Int. Ed.* **43** 5048

Liu X, Huang C, Yi S, Xie G, Li H and Luo Y 2007 *Solid State Commun.* **144** 259

Liu X H, Xie G Y, Huang C, Wu H Z and Luo Y B 2007 *Chem. Lett.* **36** 1366

Lopez R, Boatner L A, Haynes T E, Haglund Jr R F and Feldman L C 2001 *Appl. Phys. Lett.* **79** 3161

Michel T, Francois T, Joseph T and Gerard L 1973 *Comptes Rendus des Seances de l'Academie des Sciences, Serie C: Sciences Chimiques* **276** 1187

Morin F J 1959 *Phys. Rev. Lett.* **3** 34

Ng S H, Chew S Y, Wang J, Wexler D, Tournayre Y, Konstantinov K and Liu H K 2007 *J. Power Sources* **174** 1032

Odani A, Pol V G, Pol S V, Koltypin M, Gedanken A and Aurbach D 2006 *Adv. Mater.* **18** 1431

Oka Y, Yao T, Yamamoto N, Ueda Y and Hayashi A 1993 *J. Solid State Chem.* **105** 271

Parkin I P and Manning T D 2006 *J. Chem. Edu.* **83** 393

Patzke G R, Krumeich F and Nesper R 2002 *Angew. Chem. Int. Ed.* **41** 2446

Rao K J, Pecquenard B, Gies A, Levasseur A and Etourneau J 2006 *Bull. Mater. Sci.* **29** 535

Sediri F and Gharbi N 2009 *Mater. Lett.* **63** 15

Sella C, Maaza M, Nemraoui O, Lafait J, Renard N and Sampeur Y 1998 *Surf. Coat. Technol.* **98** 1477

Shi S, Cao M, He X and Xie H 2007 *Cryst. Growth Des.* **7** 1893

Strelcov E, Lilach Y and Kolmakov A 2009 *Nano Lett.* **9** 2322

Su Q, Huang C K, Wang Y, Fan Y C, Lu B A, Lan W, Wang Y Y and Liu X Q 2009 *J. Alloys Compd.* **475** 518

Sun D, Kwon C W, Baure G, Richman E, Maclean J, Dunn B and Tolbert S H 2004 *Adv. Funct. Mater.* **14** 1197

Sun X and Li Y 2004 *Angew. Chem. Int. Ed.* **43** 597

Sun X M, Liu J F and Li Y D 2006 *Chem. Mater.* **18** 3486

Theobald F and Cabala R 1970 *Comptes Rendus des Seances de I'Academie des Sciences, Serie C: Sciences Chimiques* **270** 2138

Wang X, Song J, Liu J and Wang Z L 2007 *Science* **316** 102

Wang Y, Takahashi K, Shang H and Cao G 2005 *J. Phys. Chem.* **B109** 3085

Wu Y, Xiang J, Yang C, Lu W and Lieber C M 2004 *Nature* **430** 61

Xuan S H, Hao L Y, Jiang W Q, Gong X L, Hu Y and Chen Z Y 2007 *Nanotechnology* **18** 1

Ye J W, Zhou L, Liu F J, Qi J, Gong W T, Lin Y A and Ning G L 2010 *J. Alloys Compd.* **504** 513

Yu L and Zhang X 2004 *Mater. Chem. Phys.* **87** 168

Zhang Y, Liu X, Xie G, Yu L, Yi S, Hu M and Huang C 2010 *Mater. Sci. Eng.* **B175** 164

Zhong Z, Wang D, Cui Y, Bockrath M W and Lieber C M 2003 *Science* **302** 1377

Zhou F, Zhao X M, Yuan C G, Li L and Xu H 2007 *Chem. Lett.* **36** 310